

to low-energy β particles, for which it may dominate over the imperfect wave-function overlap mechanism. However, only partial agreement with the experimental electron-electron coincidence results could be attained. On the other hand, the electron-electron coincidence results are in qualitative agreement with the calculations reported in Sec. II 2, with the possible exception of the increase in ionization probability with Z .

IV. CONCLUDING REMARKS

Clearly, further experiments on the interesting subject of the interactions between the atomic and nuclear parts of the atom during β decay would be useful. Results of the present work on β -energy dependence of internal ionization, together with total internal ionization probabilities measured by others and by us, constitute a body of data that cannot be explained by the "direct-collision" mechanism nor by the traditional wave-function overlap theory. However, it has been

shown here that the imperfect wave-function overlap theory can be improved by taking phase-space considerations into account, using relativistic electron wave functions in the calculation of the transition matrix elements, antisymmetrizing the final-state vector, and considering the allowed or forbidden character of the transitions. With these improvements, the theory agrees extremely well with available experimental results. The extent of the agreement is all the more surprising since only hydrogenic wave functions have been used and no screening corrections were made.

ACKNOWLEDGMENTS

We are indebted to many colleagues for helpful conversations; in particular, we wish to thank I. E. McCarthy and R. L. Zimmerman. We are grateful to S. P. Granados for much technical help, and to V. O. Kostroun, who kindly checked some of the calculations. We thank A. G. Fowler of the University of British Columbia Computing Center for advice on programming.

Prompt Neutron Emission from U^{235} Fission Fragments

E. E. MASLIN, A. L. RODGERS, AND W. G. F. CORE

United Kingdom Atomic Energy Authority, Aldermaston, Berkshire, England

(Received 13 June 1967)

A description is given of measurements of the prompt neutron emission from fission fragments of U^{235} in thermal neutron induced fission. A beam of neutrons from the AWRE research reactor HERALD induces fissions in a thin ($20 \mu\text{g}/\text{cm}^2$) sample of U^{235} . Neutrons are detected in a large (250 liters) liquid-scintillation counter and the fragment kinetic energies are measured with gold-silicon surface-barrier counters. Distributions, showing the neutron emission from both individual fission fragments and pairs of fragments, are given as functions of both the mass of the fragment and the total kinetic energy of the pair.

1. INTRODUCTION

PROMPT neutron emission from fission fragments provides valuable information relating to the energy balance in the fission process. The detailed shape of the curve connecting neutron emission with fragment mass number is believed to be connected directly^{1,2} with the deformability of the fragments and in particular with the near-spherical shape of fragments containing numbers of neutrons and protons near to magic numbers, and indeed the deformability parameter for various nuclear species can be calculated directly from the experimental data.² The neutron emission from the fragments, considered as an indicator of the fragment excitation energy, is thus related more to the properties of the fragments than to the mass ratio of fragment division.

The most recent data for U^{235} are those of Apalin *et al.*,³ and of Milton and Fraser.⁴ While agreement as to the general shape of the curve is obtained from these two sets of data, considerable divergencies exist as to the exact magnitude of the neutron emission ranging from 30% difference in regions of mass number 95 to approximately 70% for mass 155.

The main difficulties in this type of work relate to mass resolution, fragment coincident counting rate, and neutron-detection efficiency. While fragment time-of-flight techniques can provide the best mass resolution, they result in a low coincident counting rate, because of the small solid angle subtended at the source. Early measurements used ion chambers to measure the fragment energies. Surface-barrier counters have adequate energy resolution and can be close to the source but

¹ J. Terrell, *Phys. Rev.* **127**, 880 (1962).

² J. Terrell, in *Symposium on the Physics and Chemistry of Fission, 1965* (International Atomic Energy Agency, Vienna, 1965), Vol. 2, p. 3.

³ V. F. Apalin, Yu. N. Gritsyuk, I. E. Kutikov, V. I. Lebedev, and L. A. Mikaelian, *Nucl. Phys.* **71**, 553 (1965).

⁴ J. C. D. Milton and J. S. Fraser, in *Symposium on the Physics and Chemistry of Fission, 1965* (International Atomic Energy Agency, Vienna, 1965), Vol. 2, p. 39.

until recently suffered from uncertainties in the energy calibration procedure because of the dependence of the calibration constants on the fragment mass. Now, however, an adequate calibration procedure has become available from the work of Schmitt *et al.*⁵ with iodine and bromine ions. Nevertheless, the inherent mass resolution using surface-barrier detectors and masses calculated from energy ratios is limited to approximately 1.6 amu because of the effect of neutron emission.¹

A large liquid-scintillation counter is an ideal neutron detector having a high intrinsic efficiency largely independent of the incident neutron energy and can subtend a large solid angle at the source.

This paper describes measurements made using a beam of neutrons from the AWRE research reactor HERALD, which induces fissions in a thin sample of U^{235} . Neutrons are detected in a large liquid-scintillation counter and the fragment energies are measured with gold-silicon surface-barrier counters. Data are presented giving the neutron emission from individual fission fragments as functions of both the mass of the fragment and the total kinetic energy of the pair.

2. EXPERIMENTAL DETAILS

Measurements were made using an unfiltered beam of neutrons from the 5 MW reactor to induce fissions in a U^{235} sample. The fissions are predominantly thermal although approximately 8% have an origin in U^{235} resonances.

Two gold-silicon surface-barrier counters and a U^{235} fissile source can be mounted at the center or at the periphery of a large, 80-cm-diam tank of gadolinium-loaded liquid scintillator. The surface-barrier counters, operating in coincidence, are placed on opposite sides of a 20- $\mu\text{g}/\text{cm}^2$ evaporated deposit of U^{235} on a 70- $\mu\text{g}/\text{cm}^2$ nickel backing. Only those fissions events for which fragments travel within $\pm 20^\circ$ of the axis of the scintillation counter, i.e., the direction of the incident neutron beam, are selected for measurement by a pair of aluminum collimators.

The scintillation counter contains approximately 250 liters of commercial scintillant type NE 323 with 0.5% by weight of gadolinium loading. Fission neutrons entering the scintillant are thermalized mainly by proton recoils in an average time of 10 μsec and are finally captured preferentially (98%) by the gadolinium nuclei. The 9 MeV of γ radiation released from each capture event produces scintillations which are detected by twelve 5-in.-diam EMI photomultiplier tubes type 9618B, which are isotropically disposed over the surface of the sphere and in intimate contact with the liquid. Losses in neutron counting rate by pulse overlap are less than 1%. The photomultipliers are operated in three banks of four tubes in a triple coincidence arrangement

⁵ H. W. Schmitt, W. M. Gibson, J. H. Neiler, F. J. Walter, and T. D. Thomas, in *Symposium on the Physics and Chemistry of Fission, 1965* (International Atomic Energy Agency, Vienna, 1965), Vol. 1, p. 531.

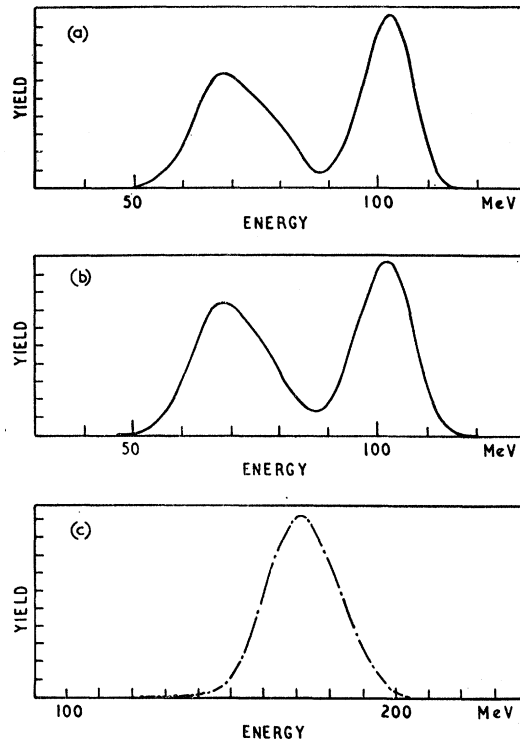


FIG. 1. Energy spectra. (a) and (b) "initial" energy spectra corrected for neutron emission; (c) total kinetic energy spectrum from both fragments.

to eliminate detection of noise pulses. The neutron pulses are recorded within a specified period following a fission event, defined as a coincidence between pulses from the two surface-barrier counters.

The arrangement has a high intrinsic efficiency (85%) for detecting fast neutrons from a fission event. However, in the present work it was necessary to operate with a gating period of 10 μsec in order to minimize the background counting rate which arose mainly from the direct scatter of the incident neutron beam by the surface-barrier counters. Under these conditions the efficiency falls to approximately 50% and the background is about 1 count per gate, while the fission fragment coincidence rate is of the order of a few per minute.

The heights of coincident pulses from the surface-barrier counters are related to the kinetic energy of each fragment and these, together with the number of scintillation pulses detected during the 10- μsec gating period, were digitized by 400-channel analog-to-digital converters and stored on paper tape.

The analysis of the data proceeds entirely with the aid of the AWRE IBM 7030 digital computer.

3. DATA

The digitized data from the three measured parameters are processed in two stages. Any long-term drifts in pulse height from the surface-barrier counters are

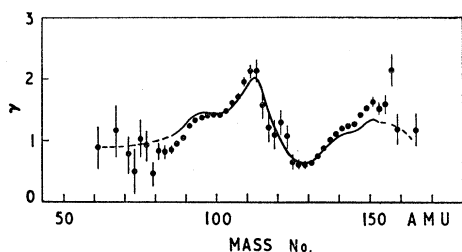


FIG. 2. Neutron emission as a function of fragment mass. The curve shows the measured neutron data before correction for the angular distribution of the neutrons with respect to the fragment direction, while the points show the data after correction.

corrected for by the computer and pulse-height spectra are produced on microfilm after every 2000 events have been processed. A visual inspection of the data is then made before the second stage of processing is undertaken.

To make an energy calibration of the pulse-height scales, the work of Schmitt *et al.*⁵ has been used. An iterative procedure is adopted to arrive at values of mass and energy for the fragments. First, a linear calibration is made by identifying the average pulse heights of the light and heavy fragments with the average energies determined using time-of-flight techniques by Milton and Fraser.⁶ An approximate mass value is then calculated using the relation $m_2 = 236 \times E_1 / (E_1 + E_2)$, where m_2 is the mass of fragment 2 and E_1 and E_2 are the respective energies of fragments 1 and 2. This mass value is then used in conjunction with data from Schmitt *et al.*⁵ to calibrate the counters by the technique described in their paper making a calibration of the form

$$E = (a + a'm)X + b + b'm,$$

where a , a' , b , b' are constants and X is the pulse height. The constants quoted by Schmitt were modified for use with average values of the light and heavy fragment groups rather than the midpoints at three quarters of the maximum peak height. A new mass value is calculated from these energies and the procedure iterated until two successive mass values are within 0.2 amu.

A first analysis of the data used these values of mass and energy to evaluate the function giving the mass dependence of the neutron emission $[\nu(m)]$ as described later. A second analysis then used the measured $\nu(m)$ curve to apply the correction calculated by Terrell¹ to transform the calculated masses to the equivalent values before neutron emission ("initial" masses).

Similar corrections were made to convert the measured energies to equivalent "initial" energies. The two initial energy spectra obtained are shown in Fig. 1 together with the total kinetic-energy spectrum. The shapes of these spectra are in excellent agreement with those of Milton and Fraser,⁶ but the average total kinetic energy, 171.5 MeV, differs from the value ob-

⁶ J. C. D. Milton and J. S. Fraser, *Can. J. Phys.* **40**, 1626 (1962).

tained by these authors, 167.6 MeV, by 3.9 MeV. The value of 171.5 MeV would be expected to be in agreement with the measurements of Schmitt *et al.*⁷ (171.9 \pm 1.4 MeV) since the same calibrations were used. The individual energy spectra are shifted by approximately 2 MeV to higher values, compared to those of Ref. 6.

A peak-to-valley ratio of 115:1 was observed in the calculated mass spectrum which compared against the radiochemical value of 650:1 shows that only about one in six of the "symmetrical fission" events are genuine.

The neutron data are processed as described in the following section using a counter efficiency, approximately 50%, which is calculated using the measured total neutron emission and normalizing to a value of ν , the average number of neutrons per fission, for U^{235} of 2.43.⁸

Two sets of data were recorded with the scintillator. In order to measure the neutron emission from individual fission fragments, a first set of data was taken with the U^{235} source placed at the periphery of the scintillation counter and the angular correlation of the prompt neutrons with fragment direction was used to associate the neutrons with the particular fragments that emitted them. A second set of data was taken with the source placed at the center of the sphere. Here the scintillation counter responds to the sum of the neutron emission from both fragments and is directly interpreted to yield the total emission as a function of fragment mass.

4. DATA ANALYSIS

The values of initial mass and energy for each event are calculated as described in the preceding section. The data are then sorted into two matrices giving both the number of events and the measured average number of

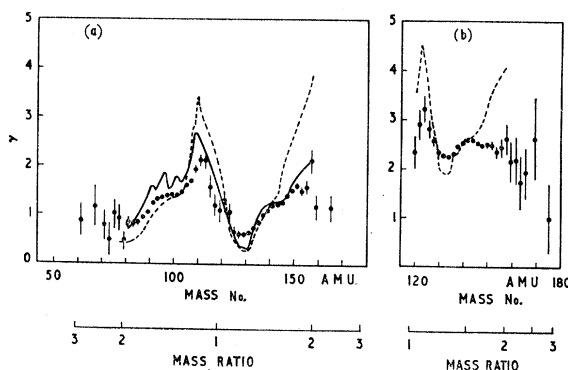


FIG. 3. (a) Neutron emission as a function of fragment mass. The points are the data from the present work; the dashed curve is the data of Apalin *et al.* (Ref. 3) and the continuous curve is the data of Fraser and Milton (Ref. 4). (b) Total neutron emission from both fragments plotted as a function of the mass of the heavy fragment; the dashed curve is the data of Apalin *et al.* (Ref. 3).

⁷ H. W. Schmitt, J. H. Neiler, and F. J. Walter, *Phys. Rev.* **141**, 1146 (1966).

⁸ C. H. Westcott, K. Ekberg, G. C. Hanna, N. J. Pattenden, S. Santani, and P. M. Attree, *At. Energy Rev.* **3**, 2 (1965).

fission neutrons for each value of fragment mass (m) and combined total fragment kinetic energy (E_T). The groupings into mass are 2 amu wide while those for the kinetic energy are 5 MeV wide.

Data from pairs of complementary masses are taken in conjunction with a matrix of calculated coefficients $P(m, E_T)$, where $1 - P(m, E_T)$ defines the probability that a fission neutron will enter the detector, to give a corrected value for the average number of prompt neutrons emitted per fragment for each value of mass and total kinetic energy. To illustrate the magnitude of the corrections involved Fig. 2 shows a comparison of the measured neutron emission corrected for background and counter efficiency with that calculated after applying the coefficients $P(m, E_T)$. These coefficients are calculated assuming isotropic emission of neutrons in the fragment frame of reference and a neutron emission spectrum of two Maxwellian terms; the resulting probabilities are integrated over the range of angles of fragment emission defined by the fragment collection geometry and weighted by the fragment angular distribution.

The spectrum assumed for these calculations is of the form

$$\phi(E_{c.m.}) = (E_{c.m.}/T^2)e^{-E_{c.m.}/T},$$

where ϕ is the probability of emission of a neutron from a nucleus of temperature T with a center-of-mass energy $E_{c.m.}$, and the combined spectra are added as

$$\phi = a_1\phi_1 + a_2\phi_2,$$

using the values of the coefficients found by Milton and Fraser⁴ to give a good fit to the laboratory spectrum. These are

$$\begin{aligned} a_1 &= 0.703, & a_2 &= 0.297, \\ T_1 &= 0.779 \text{ MeV}, & T_2 &= 0.287 \text{ MeV}. \end{aligned}$$

The probability coefficients $P(m, E_T)$ are defined

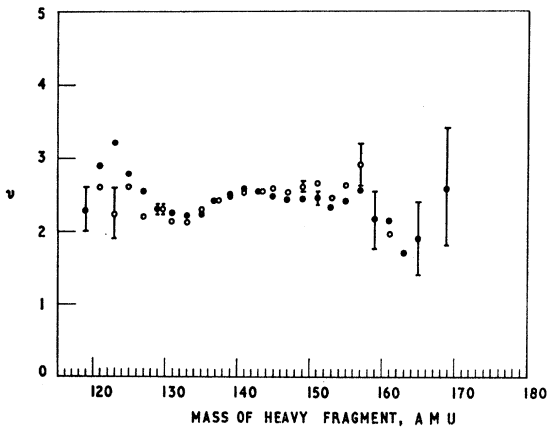


FIG. 4. Comparison of total neutron emission from fragment pairs as a function of mass of the heavy fragment. The full dots are the sums of values from the two separate fragments while the open circles are data measured directly with the U^{235} foil at the center of the scintillator.

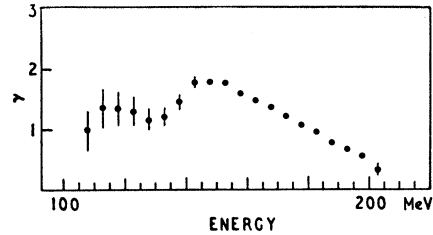


FIG. 5. Average neutron emission per fragment as a function of total kinetic energy of both fragments.

above. Now, let

$$p(v_f, v_n, \theta) = \frac{1}{2}(1 - v_f \cos\theta/v_n),$$

where v is the center-of-mass velocity of fragments, v_n is the center-of-mass velocity of neutron, and θ is the angle of neutron emission with respect to the axis of the scintillator. Then

$$P(m, E_T) = \int_0^{\pi/2} \int_0^{\infty} v_f \cos\theta p(v_f, v_n, \theta) \times f(v_n) \times g(\theta) dv_n d\theta,$$

where $f(v_n)$ is the velocity distribution function equivalent to the energy spectrum given above and $g(\theta)$ is the angular distribution of fragments accepted by the collimation system.

The number and neutron-number matrices enable information on the mass and total kinetic-energy spectra and on the neutron emission to be obtained. In particular, by summing and averaging the matrix of neutron numbers along the total kinetic energy coordinate, average values of neutron emission as a function of fragment mass are obtained. Also, sums of pairs of neutron-emission values for complementary masses provide the total average ν for the pair of fragments as a function of mass ratio, which is to be compared to the directly measured values referred to in Sec. 3.

5. RESULTS AND DISCUSSION

The neutron distribution as a function of mass number appears in Fig. 2. The essential characteristics of the distribution are found to be the same as in previous work [see Fig. 3(a), Refs. 3 and 4], but there is no evidence of the high neutron-emission values 3.5 to 4, at mass numbers 110 and 156, observed by Apalin *et al.*³ The fine structure seen by Milton and Fraser⁴ at masses 90, 96, and 101 is not visible in these data, presumably because of the poorer mass resolution in double-energy experiments compared to time-of-flight work. The general shape of the curve is as has been predicted by the statistical partition of energy between the fragments.⁹

The ratio of ν_L/ν_H is 1.27 ± 0.05 compared to 1.49 calculated from the data of Ref. 4, using the fits given by the parameters quoted in Sec. 4 and compared to

⁹ E. Erba, U. Faccini, and E. Saetta-Menichella, Nucl. Phys. 84, 595 (1966).

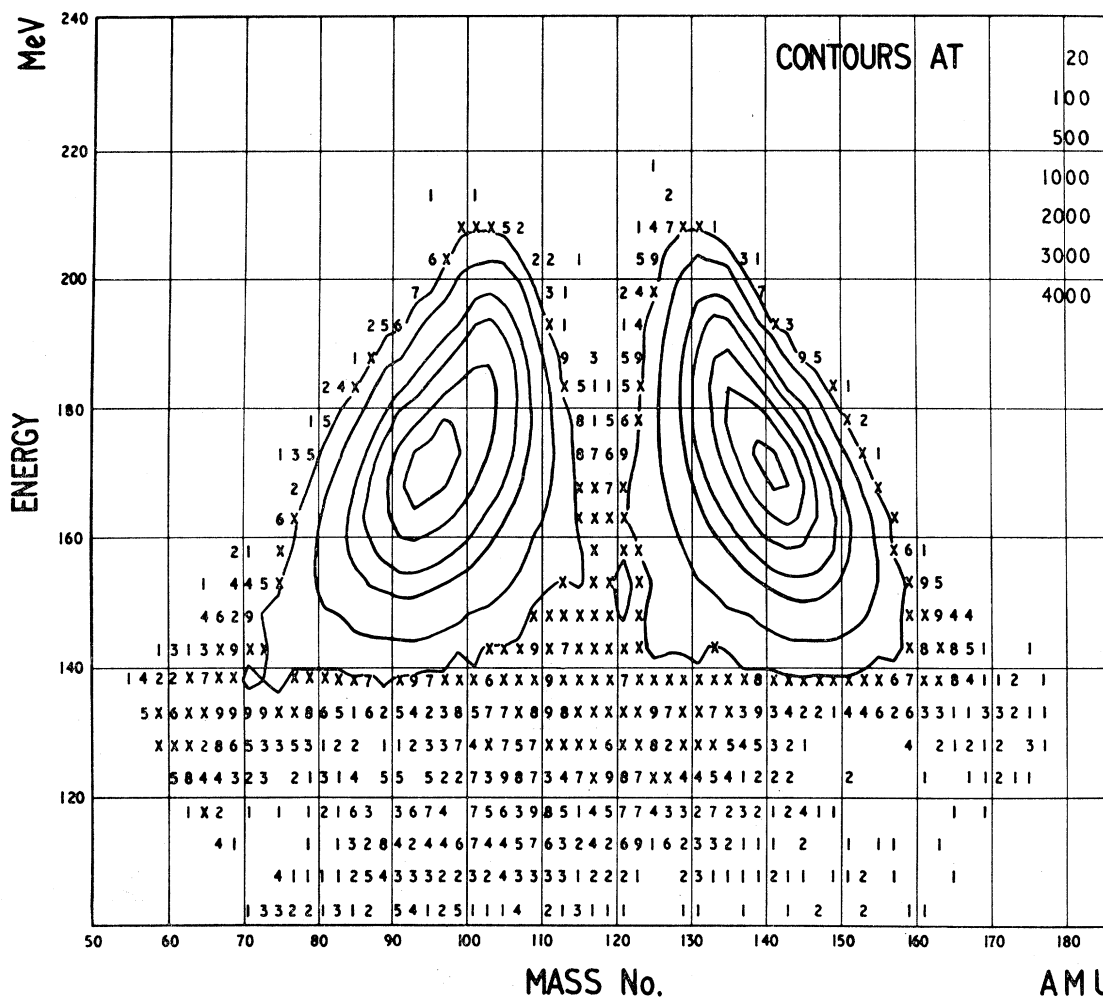


FIG. 6. Contour diagram showing the distribution of measured events as a function of both fragment mass and total kinetic energy of both fragments. The individual numbers show the number of events recorded in each cell, $5 \text{ MeV} \times 2 \text{ amu}$, where this is below 10. The symbol X denotes a number between 10 and 20.

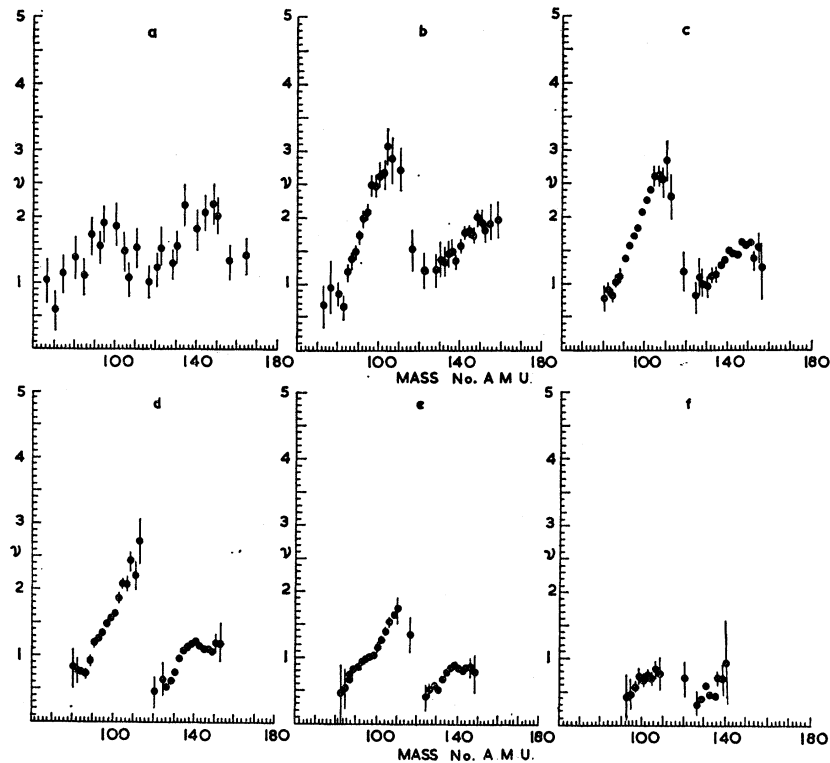
1.15 ± 0.07 in the work of Apalin *et al.*¹⁰ These values are sufficiently different from unity to argue against the suggestion of Terrell¹ that the neutron emission from the light and heavy fragments is the same.

In Fig. 3(b) the total neutron emission obtained by summing the individual values for pairs of fragments is plotted as a function of mass of the heavy fragment, while Fig. 4 compares these data with those measured directly with the source at the center of the scintillation counter. The agreement between the two sets of data is good except perhaps in the region near symmetrical fission. The area of agreement suggests that the systematic errors associated with the corrections that were necessary in calculating the indirect set of data are small and gives more confidence to these data; it suggests that in this region the errors in the values of ν for different mass values are of the order of ± 0.05 neutron.

¹⁰ V. F. Apalin, Yu. N. Gritsyuk, I. E. Kutikov, V. I. Lebedev, and L. A. Mikaelian, *Nucl. Phys.* **55**, 249 (1964).

Referring again to Fig. 3(b), which also shows the data of Apalin *et al.*,³ we see that the pronounced minimum in the mass region 131 is confirmed, and there is a tendency for the curve to rise as symmetry is approached although the values plotted at mass ratios approaching unity are necessarily averages over a range of values, since no more than $\frac{1}{6}$ of the symmetrical events are believed to be genuine (see Sec. 3). The dip at symmetry is due to the inclusion of events of lower than average kinetic energy and which are associated with a lower value of neutron emission (see below and Fig. 5). The comparison with the data of Apalin *et al.*³ shows similar characteristics, but beyond mass 140 there is disagreement. The Apalin curve shows a strong rise beyond mass 150, whereas our curve tends to decrease. Comparison of our data with those of Terrell¹ obtained from cumulative mass yields reveals an excellent agreement in the region covered by that data, namely, heavy masses 130 to 153 amu; the slight

FIG. 7. Mass dependence of neutron emission for various kinetic energy groups. Energy groups are (a) 103 to 143 MeV, (b) 148 to 153 MeV, (c) 158 to 163 MeV, (d) 168 to 173 MeV, (e) 178 to 188 MeV, (f) 193 to 238 MeV.



downward trend towards the high mass numbers is apparent in both sets of data.

Figure 5 illustrates the average neutron emission per fragment, averaged over the mass distribution and plotted as a function of the total kinetic energy of the fragments. If we consider the linear part of this curve and allow for emission from both fragments, then $dE_T/d\nu = 18.5$ MeV/ n , where E_T is the total kinetic energy and ν is the total neutron emission from both fragments. This is considerably higher than the figure of 6.6 MeV/ n obtained by Bowman *et al.*¹¹ in similar studies of Cf^{252} fission fragments. The kinetic energies can be converted into fragment excitation energies using the energy releases calculated by Milton¹² from the Cameron mass formula.¹³ In general, no large differences are observed in the shapes of curves of ν versus E , whether excitation energies or kinetic energies are used. The value of $dE^*/d\nu$ becomes 15.2 MeV/ n , which should be compared with an average figure of about 25 MeV/ n calculated from the data of Milton and Fraser.⁴ Our value implies that as much of the excess energy might be liberated in the form of γ radiation as is released by prompt neutron emission.

The lower neutron emission observed at about 120 MeV in Fig. 5 is of some interest. The events corresponding to these data are best illustrated in Fig. 6,

¹¹ H. R. Bowman, J. C. D. Milton, S. G. Thompson, and W. J. Swiatecki, *Phys. Rev.* **129**, 2133 (1963).

¹² J. C. D. Milton, University of California, Lawrence Radiation Laboratory Report No. UCRL-9883, 1962 (unpublished).

¹³ A. G. W. Cameron, *Can. J. Phys.* **35**, 1021 (1957).

where they form a group of events below the main body of data. The events appear similar to the "energy tails" reported by Apalin *et al.*¹⁴ In view of the completely different experimental apparatus employed in their work, it would be hard to consider that the "tails" were due to a spurious experimental effect if it were not for the data of Schmitt *et al.*,⁷ in which only a negligible number of events appear in this region. Any spurious degradation of energy of one of the fragments sufficient to shift the combined energy by greater than 40 MeV would lead to an abnormal calculated value of mass; only if both fragments were proportionately degraded would the calculated mass value remain unaltered. However, in view of the data of Schmitt *et al.*, we suspect these events may be spurious although the cause of energy degradation is uncertain. If they correspond to events with degraded energy, the neutron emission from them would be expected to be about the average value which is seen to be the case in Fig. 5. These events are responsible for an abnormally low value of total kinetic energy observed at symmetrical fission. We find a "dip" of 33 MeV between the kinetic energy values at 118 and 132 amu and if a rather arbitrary deletion of the degraded events is made, this "dip" becomes only 22 MeV. This should be compared to values of 21 MeV obtained by Apalin *et al.*¹⁴ after deleting the "spurious" events observed in their work and

¹⁴ V. F. Apalin, Yu. N. Gritsyuk, I. E. Kutikov, V. I. Lebedev, and L. A. Mikaelian, *Nucl. Phys.* **71**, 546 (1965).

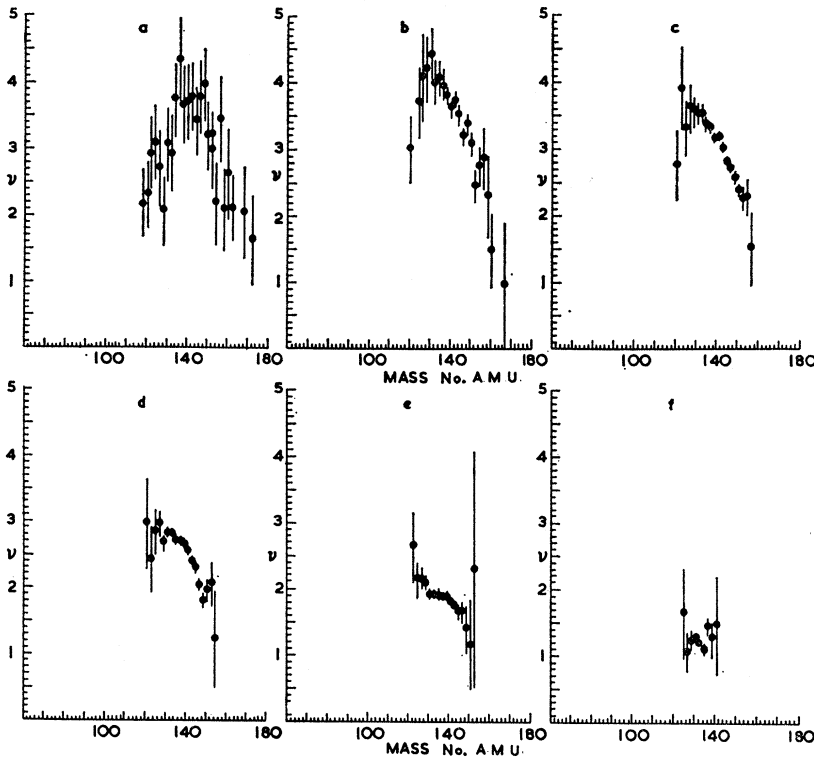


FIG. 8. Total neutron emission from both fragments for the same energy groups as Fig. 7.

a value in the range 18–27 MeV obtained by Alexander *et al.*¹⁵ by measurements of fragment ranges.

The full data describing the neutron emission as a function of both fragment mass and total kinetic energy are available as a matrix, stored on punched cards, and are printed in full in Ref. 16. However, some interesting features of the data can be seen from the sets of figures showing subdivision of the data in various ways, Figs. 7–9. Figure 7 illustrates the mass dependence of neutron emission for various kinetic energy groups. Graph (a) in this set refers mainly to the events of abnormally low kinetic energy referred to above. The remaining graphs exhibit the general shape of Fig. 3 with the average value of neutron emission steadily decreasing with excitation energy, that is, increasing with kinetic energy. A change of slope of the curve is observed at about 140 amu which is particularly prominent in graphs (d) and (e). A similar flattening has been previously observed in the neutron emission from Cf^{252} fission fragments in the work of Bowman *et al.*¹¹ This is the beginning of a region of nuclei with large quadrupole moments¹⁷ indicating nuclei with stable ground-state deformations. The work of Kapoor, Bow-

man, and Thompson¹⁸ in studies of x-ray emission from fission fragments of Cf^{252} has indicated an increase in internally converted x-ray emission from fragments with masses greater than 140 amu. These pieces of evidence suggest that the excitation energy of these fragments is released by de-excitations from the levels of the deformed nuclei through low-energy γ -ray transitions rather than by neutron emission.

Figure 8 shows the total neutron emission from the pair of fragments for the same fragment kinetic-energy groups as Fig. 7. Here, the shape of the curves are not the same as in Fig. 3(b); for example, the minimum in Fig. 3(b) at mass 132 is not apparent in any of the subgroups except perhaps graph (e), where a slight discontinuity is seen. The minimum is apparently formed by the overlap of these several graphs.

A feature of these graphs is the maximum in neutron emission in the region of asymmetric fission, and it is interesting to note that the statistical theory of fission¹⁹ predicts an increase in excitation energy and therefore neutron emission for the asymmetric modes.

Figure 9 shows the variation of neutron emission with total fragment kinetic energy for several mass groups. The curves plot ν versus E_T but only small differences in shape are observed if E^* values are substituted. The character of the curves is much the same as Fig. 5 although the slopes of the linear portions

¹⁵ J. M. Alexander, M. F. Gazdik, A. R. Trips, and S. Wasif, *Phys. Rev.* **129**, 2659 (1963).

¹⁶ E. E. Maslin, A. L. Rodgers, and W. G. F. Core, Atomic Weapons Research Establishment Report No. 0-43/67, 1967 (unpublished).

¹⁷ W. D. Myers and W. J. Swiatecki, University of California, Lawrence Radiation Laboratory Report No. UCRL-11980, 1965 (unpublished).

¹⁸ S. S. Kapoor, H. R. Bowman, and S. G. Thompson, *Phys. Rev.* **140**, B1310 (1965).

¹⁹ P. Fong, *Phys. Rev.* **102**, 434 (1956).

FIG. 9. Average neutron emission per fragment versus total kinetic energy of both fragments, plotted for various mass groupings. Mass groups are: (a) 51 to 89 amu, (b) 91 to 103 amu, (c) 105 to 117 amu, (d) 119 to 131 amu (e) 133 to 145 amu, (f) 147 to 185 amu.

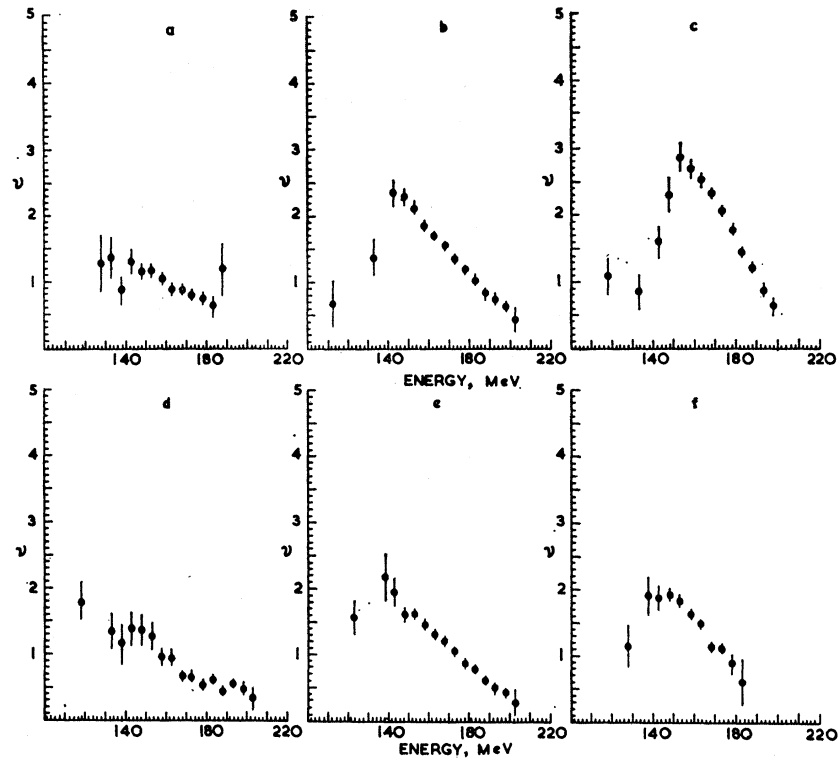
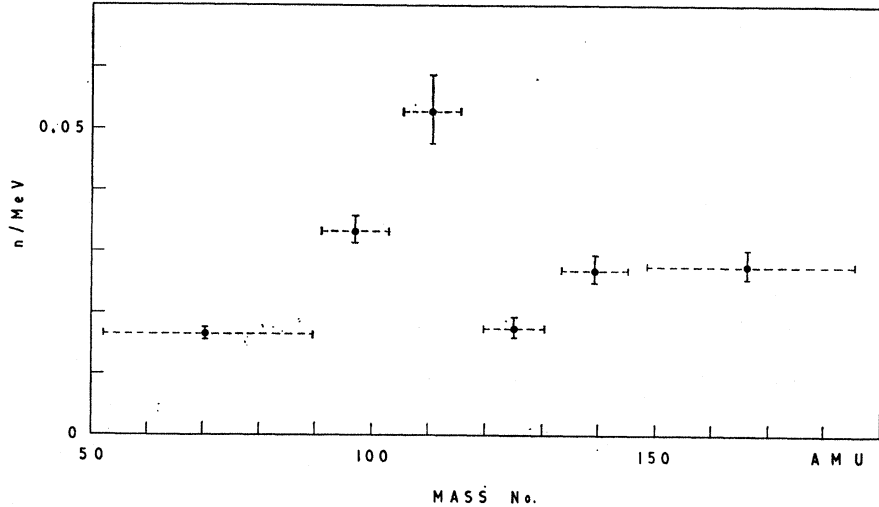


FIG. 10. Slopes of linear portions of graphs in Fig. 9 plotted as a function of fragment of mass. The horizontal lines indicate the width of the mass groups used to calculate each point.



show a distinct variation. Figure 10 shows the values of the slopes dv/dE_T for complementary fragment masses. It is seen from this figure that, for a given level of total excitation energy, the neutron emission from the fragment pairs at 110, 125 amu and at 97, 139 amu is more than that from the fragment pair at 70, 165 amu. This raises the possibility that the extra excitation energy in the latter mode is released in the form of γ radiation and is consistent with the conclusion that was made earlier that low-energy γ -ray transitions pre-

dominate over neutron emission beyond about 140 amu.

We have performed the same analysis on the data taken with the source at the center of the tank, that is, referring to neutron emission from both fragments, and find that the curves show similar characteristics to those of Figs. 8 and 9; such differences as there are can be accounted for by small differences in the groups of events selected. The individual curves are available in Ref. 16.